A&A 447, 379–387 (2006)
DOI: 10.1051/0004-6361:20053737
© ESO 2006

Astronomy & Astrophysics

Dielectronic recombination data for dynamic finite-density plasmas

IX. The fluorine isoelectronic sequence

O. Zatsarinny[1,⋆], T. W. Gorczyca[1], J. Fu[1], K. T. Korista[1], N. R. Badnell[2], and D. W. Savin[3]

[1] Department of Physics, Western Michigan University, Kalamazoo, Michigan, 49008-5252, USA
e-mail: [gorczyca;korista]@physics.wmich.edu
[2] Department of Physics, University of Strathclyde, Glasgow, G4 0NG, UK
[3] Columbia Astrophysics Laboratory, Columbia University, New York, NY 10027-6601, USA
e-mail: savin@astro.columbia.edu

Received 30 June 2005 / Accepted 27 July 2005

ABSTRACT

Partial and total dielectronic recombination (DR) rate coefficients for fluorine-like ions forming neon-like systems have been calculated as part of the assembly of a final-state level-resolved DR database necessary for the modelling of dynamic finite-density plasmas (Badnell et al. 2003). Calculations have been performed for DR of both ground and metastable initial states for Ne^{+} to Zn^{21+}, as well as for Kr^{27+}, Mo^{33+}, and Xe^{45+}. Results for a selection of ions are presented and discussed. We find that low-temperature DR, via $2 \rightarrow 2$ core excitations involving no change in the principal quantum number of the core electron, does not scale smoothly with nuclear charge Z due to resonances straddling the ionization limit of the recombined system, thereby making explicit calculations for each ion necessary. Most of the earlier calculations neglected contributions from the fine-structure $2p_{3/2} - 2p_{1/2}$ excitation which has been shown to be very important for low-temperature DR coefficients. The DR data are suitable for modelling of solar and cosmic plasmas under conditions of collisional ionization equilibrium, photoionization equilibrium, and non-equilibrium ionization.

Key words. atomic data – atomic processes – plasmas

1. Introduction

Dielectronic recombination (DR) is an important recombination process for laboratory and astrophysical plasmas. Accurate DR coefficients are essential in the determination of the ionization balance and in the interpretation of most types of astrophysical spectra. The DR process has been subject to intense theoretical study, but the existing sophisticated calculations have been done only for specific ions, and most available data are based on simplified models. Recently, a critical evaluation of the uncertainties of the existing theoretical high-temperature DR rate coefficients for electron ionized plasmas was performed by Savin & Laming (2002). It was found that the uncertainties can be as large as a factor of 2–5 for some ions. The published high-temperature DR rate coefficients for fluorine-like ions vary by up to a factor of 4.7. Recent experimental measurements (Savin et al. 1997, 1999, 2002a,b, 2003; Schippers et al. 2001, 2004) have also shown that many of the earlier computations of low temperature DR rate coefficients are inaccurate. Taken altogether, it is clear that systematic computations with improved approximations are needed. Most of the earlier calculations neglected the contributions from the fine-structure $2p_{3/2}$–$2p_{1/2}$ excitation which has been shown to be very important for low-temperature DR coefficients. Including fine-structure excitations is thus essential for producing reliable DR rate coefficients applicable to modelling of photoionized plasmas.

We have initiated a program to generate an initial and final-state level-resolved intermediate coupling DR database necessary for spectroscopic modelling of dynamic and/or finite density plasmas (Badnell et al. 2003). To this end, work has been underway in the calculation of DR data for the hydrogen through magnesium-like isoelectronic sequences and beyond. Recent papers cover the N-like (Mitnik & Badnell 2004), Ne-like (Zatsarinny et al. 2004) and B-like (Altun et al. 2004) isoelectronic sequences, and contain references to earlier papers/sequences. In this paper, we describe calculations and results for dielectronic recombination data for fluorine-like ions forming neon-like ions. This sequence has been shown to be

⋆ *Present Address*: Physics Department, Drake University, Des Moines, IA 50311, USA e-mail: oleg_zoi@yahoo.com

Article published by EDP Sciences and available at http://www.edpsciences.org/aa or http://dx.doi.org/10.1051/0004-6361:20053737

important in the determination of solar and stellar upper atmosphere abundances (Savin & Laming 2002).

Although studies for a few elements of this sequence have been made, there are no systematically determined DR rate coefficients for the entire sequence. The first calculations of DR rate coefficients for fluorine-like ions appear to be those of Jacobs et al. (1977, 1979, 1980) and Jacobs (1985) for Ne, Mg, Na, Si, S, Ca, Fe, and Ni atoms using a simplified model. In this model, the autoionization rates were obtained from the threshold values of the partial-wave electron-impact excitation cross sections for the corresponding one less charged systems by means of the quantum-defect theory relationship between these values. The excitation cross sections were obtained in the distorted-wave approximation in LS coupling, and only dipole 2s−2p, 2p−3s, and 2p−3d transitions were included. In addition, radiative decay of autoionizing states was approximated as the ionic core radiative decay rate. As we will discuss, this simplified model gives fairly accurate high-temperature DR rate coefficients for low-charged Mg^{3+}, but underestimates DR rate coefficients for the heavier Si^{5+}, S^{7+}, and Fe^{17+} ions by large factors at the peak in the DR rate coefficient.

Roszman (1987) performed more detailed DR calculations, and presented rate coefficients for the Ar^{9+}, Fe^{17+}, Kr^{27+}, and Mo^{33+} ions. A frozen-core model of the atomic structure, with single-configuration LS coupling, and distorted-wave approximations, were used to compute the orbital energies, the radiative transition rates, and the autoionization rates. Roszman included all $2 \rightarrow 2$ and $2 \rightarrow 3$ dipole-allowed radiative transitions which lead to recombination. The numerical results for low-n contributions were extrapolated to the $n = \infty$ limit as needed for the computation of the total DR rate coefficients. Roszman also provided an analytic interpolation formula for estimating the DR rate coefficients for ions in between those calculated.

Detailed calculations using a Hartree-Fock (HF) method that includes relativistic corrections, but not configuration interactions, were carried out for Ar^{9+}, Ti^{13+}, Fe^{17+} and Se^{25+} by Dasgupta & Whitney (1990). Three- and four-parameter fits were then made to these data and it was suggested that these fitting formulae would enable one to obtain DR rate coefficients for all elements in the fourth row of the periodic table by a combination of interpolation and extrapolation. As we show below, the low-temperature DR rate coefficients of F-like ions have very irregular behavior, so that interpolation (or extrapolation) from some actually calculated elements to other elements is unsafe. In order to obtain reliable results, one should perform calculations for all elements under consideration.

A sophisticated study of DR rate coefficients for six fluorine-like ions with atomic number $26 \leq Z \leq 63$ has been performed by Chen (1988). The calculations were carried out in the isolated resonance approximation for temperatures in the range $0.01 \leq T \leq 9$ keV. The Auger and radiative rates for each autoionizing state were computed explicitly by use of the multiconfiguration Dirac-Fock (MCDF) method in intermediate coupling and including configuration interaction. Comparison with previous results of Roszman (1987) shows large discrepancies which were attributed to the numerical errors in the Roszman data. Note that the calculations of Jacobs et al. (1977, 1979, 1980), Jacobs (1985), Roszman (1987), Dasgupta & Whitney (1990), and Chen (1988) all neglected the contributions from the fine-structure $2p_{3/2}$–$2p_{1/2}$ excitation of the recombining ions.

The available DR data for the fluorine-like sequence were fitted by Mazzotta et al. (1998), and the results were tabulated for all fluorine-like ions from Ne^{+} to Ni^{19+}. For low-charged ions they used the results from the simplified model calculations of Jacobs et al. (1977, 1979) as fitted by Shull & Van Steenberg (1982); and for atoms from Ar to Ni they adopted the fitting formula of Dasgupta & Whitney (1990). As shown below, this compilation of Mazzota et al. (1998) contains DR rate coefficients which differ by as much as a factor of 2 from the most recent theoretical and experimental data for fluorine-like ions.

Very recently, new investigations of the DR rate coefficients for H-like through Ne-like isosequences of Mg, Si, S, Ar, Ca, Fe, and Ni have been presented by Gu (2003). The data were produced by the Flexible Atomic Code (FAC), a newly developed relativistic, multiconfiguration atomic code similar to HULLAC (Bar-Shalom et al. 2001). The atomic structure is solved in the configuration interaction approximation with basis states constructed using the Dirac-Fock-Slater method. The continuum processes are treated in the distorted-wave approximation. Resonant processes such as DR and resonance excitation are treated in an independent processes, isolated resonance approximation. The results of Gu (2003) show large discrepancies with existing DR rate coefficients for F-like ions in the low temperature region. A comparison with this new data of Gu (2003) thus provides a good opportunity to check the reliability of both calculations for the fluorine isoelectronic sequence.

The first high-resolution measurement of DR on a fluorine-like ion was done by Lampert et al. (1996). They measured the DR cross section of Se^{25+} at center-of-mass energies from 1 to 1800 eV using merged electron-ion beams in the Heidelberg heavy-ion Test Storage Ring (TSR) facility. All dielectronic resonances involving changes of $\Delta N = 0$ and $\Delta N = 1$ of the core principal quantum number N were covered with high-energy resolution. A strong contribution of the $\Delta N = 1$ resonances at 1200−1700 eV was observed. Comparison was made with isolated-resonance intermediate-coupling calculations carried out using the multiconfiguration Breit-Pauli (MCBP) code AUTOSTRUCTURE (Badnell 1986; Badnell & Pindzola 1989). Good agreement was found for the $\Delta N = 0$ and the low-lying $\Delta N = 1$ resonances. For the $\Delta N = 1$ Rydberg series, the resonant pattern continues to be well reproduced by theory, but the total theoretical energy-integrated cross section falls below the measurements by about 20%. This is somewhat greater than the quoted total experimental uncertainty of 15%.

Precise experimental measurements with high resolution have also been performed using TSR for fluorine-like Fe^{17+} by Savin et al. (1997, 1999) for DR via $N = 2 \rightarrow N' = 2$ core excitation, also using the TSR. Significant discrepancies were found between experimentally derived rate coefficients and previously published theoretical results. In specific, the previous calculations did not account for DR via $2p_{3/2} \rightarrow 2p_{1/2}$ fine structure core excitation. This can play a significant role in the

DR process at low temperatures such as are important in photoionized plasmas. Hence, the measurements call into question all previous theoretical $2 \rightarrow 2$ DR rate coefficients used for ionization balance calculations of photoionized cosmic plasmas. In the work of Savin et al. (1997, 1999), new theoretical calculations were also carried out using MCBP and multiconfiguration Dirac-Fock (MCDF) methods. These new theoretical results yielded good agreement with experiment, mainly due to inclusion of $2p_{3/2}$–$2p_{1/2}$ core fine-structure excitations.

In this paper, we apply an intermediate-coupling, MCBP method, in the isolated resonance approximation, to compute DR rate coefficients for all fluorine-like ions from Ne^{+} to Zn^{21+}, and also for the highly-charged ions Kr^{27+}, Mo^{33+}, and Xe^{45+}. The rate coefficients detailed here cover a wide range of temperatures and ionic species, and are expected to be more accurate than the results produced by earlier calculations based on cruder approximations.

The present work archives final state-resolved DR coefficients, which are necessary for modelling plasmas at densities for which the coronal approximation is not valid, for both the ground and metastable initial states. This is necessary for modelling dynamic plasmas whose metastable populations are not in quasi-static equilibrium with the ground state. Total (zero-density) DR rate coefficients from the ground state are also presented in compact form using a simple fitting formula. Data are presented for each ion, since the large irregularity in Z-dependence of the total DR rate coefficients at low temperatures makes scaling inaccurate. It is impractical to list all level-resolved rate coefficients in a paper publication. As previously discussed (Badnell et al. 2003), the present data will form part of an Atomic Data and Analysis Structure (ADAS) dataset comprising the *adf09* files for each ion, detailing the rate coefficients to each LSJ-resolved final state. This is available through the ADAS project (Summers 2003) and is also made available online at the Oak Ridge Controlled Fusion Atomic Data Center `http://www-cfadc.phy.ornl.gov/data_and_codes`.

The rest of this paper is organized as follows: in Sect. 2 we give a brief description of the theory used and the details of our calculations for the fluorine-like ions. In Sect. 3 we present results for the total DR rate coefficients for 24 ions in this sequence. We conclude with a brief summary in Sect. 4.

2. Theory

Details of our calculations have already been described elsewhere (Badnell et al. 2003). Here we outline only the main points. DR cross section calculations were carried out using the code AUTOSTRUCTURE (Badnell 1986; Badnell & Pindzola 1989), which is based on lowest order perturbation theory, where both the electron-electron and electron-photon interactions are treated to first order. This independent-processes, isolated-resonance approximation is used to calculate configuration-mixed LS and IC energy levels, radiative rates, and autoionization rates, which are then used to compute Lorentzian DR resonance profiles. This enables the generation of final-state level-resolved and total DR rate coefficients.

The DR process for fluorine-like ions can be represented, in intermediate coupling, as

$$\mathrm{A}^{q+}(2s^2 2p^5[^2P_{3/2}]) + e^- \rightarrow \begin{cases} \mathrm{A}^{(q-1)+}(2s^2 2p^5[^2P_{1/2}]nl) \\ \mathrm{A}^{(q-1)+}(2s2p^6[^2S_{1/2}]nl) \end{cases} \quad (1)$$

for $2 \rightarrow 2$ core excitation, where we included all $0 \le l \le 15$ and $3 \le n \le 1000$. For $2 \rightarrow 3$ core excitation, the DR process can be written as

$$\mathrm{A}^{q+}(2s^2 2p^5[^2P_{3/2}]) + e^- \rightarrow \begin{cases} \mathrm{A}^{(q-1)+}(2s^2 2p^4 3lnl') \\ \mathrm{A}^{(q-1)+}(2s2p^5 3lnl') \\ \mathrm{A}^{(q-1)+}(2p^6 3lnl') \end{cases} \quad (2)$$

with $0 \le l \le 6$ and $3 \le n \le 1000$ (higher-l DR drops off faster in this case).

A bound orbital basis (1s, 2s, 2p, 3s, 3p, 3d) was generated from a configuration-average Hartree-Fock (Froese Fischer 1991) calculation for the $1s^2 2s^2 2p^5$ configuration to get the first three orbitals, followed by a configuration-average, frozen-core HF calculation for the $1s^2 2s^2 2p^4 3l$ states to get the additional $n = 3$ orbitals. Then the corresponding atomic structures for both initial-ion states and resonance and bound states of the recombining ion were obtained by diagonalizing the appropriate Breit-Pauli Hamiltonian. All target states were obtained with full configuration and term mixing of configurations indicated in Eqs. (1) and (2). Prior to the final DR cross section calculations, the ionic thresholds for the $N = 2$ target states were shifted to the known spectroscopic values (`http://physics.nist.gov/cgi-bin/AtData/main_asd`) by a small amount – typically in the range of 1–2 eV for high Z. Distorted wave calculations were then performed to generate the appropriate free εl and bound nl ($n > 3$) orbitals which are attached to each target state to yield the continuum and resonance states, respectively. All of the above orbitals are computed in the absence of any relativistic effects. However, the continuum and resonance states are subsequently recoupled to an intermediate coupling scheme in order to include relativistic effects to lowest order. Also, DR contributions from the $3l3l'$ autoionizing states are considered separately with full configuration and spin-orbit mixing.

The DR data is a sum of Lorentzian profiles and can therefore be convoluted analytically with the experimental energy distribution, in order to compare to measured results, or with a Maxwellian electron distribution, in order to obtain total DR rate coefficients. This represents a huge savings in computational effort over R-matrix calculations since the latter must be performed for an extremely dense energy mesh in order to fully resolve all resonances (Gorczyca et al. 2002; Ramirez & Bautista 2002). The total DR rate coefficients were then fitted using

$$\alpha_{\mathrm{DR}}(T) = T^{-3/2} \sum_i c_i e^{-E_i/T} \quad (3)$$

in order to facilitate the further application of our data. Here, the electron temperature T and the energy fitting parameter E_i are in units of eV, and the rate coefficient $\alpha_{\mathrm{DR}}(T)$ is in units of 10^{-11} cm^3 s^{-1} (which fixes the units of c_i). Table 1 lists the

Table 1. Fitting coefficients of Eq. (3) for dielectronic recombination of F-like ions forming Ne-like systems. The c_i are in units of 10^{-11} cm^3 s^{-1} eV$^{3/2}$ and the E_i are in eV.

Ion	c_1	c_2	c_3	c_4	c_5	c_6	c_7
Ne^{+}	3.322E−04	3.725E−04	1.048E−03	1.134E−04	6.374E+01	1.017E+00	0.000E+00
Na^{2+}	2.205E−03	6.475E−03	6.765E−03	1.370E+02	7.026E+01	3.303E−01	0.000E+00
Mg^{3+}	7.520E−03	3.054E−02	1.651E−02	2.168E+00	3.042E+02	2.469E+02	0.000E+00
Al^{4+}	2.590E−02	9.216E−02	1.869E−01	5.527E−01	1.540E+02	4.065E+02	7.454E+02
Si^{5+}	4.858E−02	2.016E−01	6.506E−02	3.515E+00	5.414E+02	1.137E+03	1.033E+03
P^{6+}	1.093E+00	4.707E−01	1.316E−01	2.136E+01	7.418E+02	2.866E+03	1.713E+03
S^{7+}	2.068E−01	7.614E−01	4.155E−01	2.972E+01	1.242E+03	8.104E+03	0.000E+00
Cl^{8+}	3.529E−01	1.338E+00	3.957E+00	5.851E+01	6.099E+02	1.765E+03	1.247E+04
Ar^{9+}	5.453E−01	2.587E+00	1.630E+01	1.750E+02	2.434E+03	2.034E+04	0.000E+00
K^{10+}	8.224E−01	3.130E+00	2.326E+00	3.565E+02	3.807E+03	2.896E+04	0.000E+00
Ca^{11+}	1.136E+00	4.312E+00	7.399E+00	4.551E+02	4.264E+03	3.962E+04	1.286E+02
Sc^{12+}	1.638E+00	6.782E+00	3.056E+01	6.620E+02	5.651E+03	5.158E+04	0.000E+00
Ti^{13+}	3.952E+00	2.173E+01	6.354E+01	1.163E+03	9.968E+03	6.288E+04	0.000E+00
V^{14+}	5.776E+00	9.296E+01	1.370E+01	1.338E+03	1.506E+04	7.428E+04	0.000E+00
Cr^{15+}	3.971E+00	1.407E+01	3.672E+01	1.522E+03	1.735E+04	8.984E+04	0.000E+00
Mn^{16+}	4.948E+00	1.766E+01	9.264E+01	1.926E+03	2.550E+04	1.011E+05	0.000E+00
Fe^{17+}	6.566E+00	2.213E+01	1.518E+02	2.274E+03	3.218E+04	1.147E+05	0.000E+00
Co^{18+}	7.908E+00	4.006E+01	2.266E+02	2.732E+03	2.994E+04	1.362E+05	0.000E+00
Ni^{19+}	1.204E+01	1.066E+02	3.266E+02	3.124E+03	3.117E+04	1.554E+05	0.000E+00
Cu^{20+}	2.026E+01	3.141E+02	1.528E+02	3.441E+03	5.040E+04	1.569E+05	0.000E+00
Zn^{21+}	2.912E+02	5.201E+01	1.978E+02	3.878E+03	9.712E+04	1.318E+05	0.000E+00
Kr^{27+}	4.556E+01	2.475E+02	1.219E+03	8.400E+03	1.283E+05	2.281E+05	0.000E+00
Mo^{33+}	1.153E+02	1.580E+03	2.174E+03	1.660E+04	1.898E+05	2.818E+05	0.000E+00
Xe^{45+}	2.422E+02	4.428E+03	6.076E+03	3.993E+04	3.563E+05	2.662E+05	0.000E+00
	E_1	E_2	E_3	E_4	E_5	E_6	E_7
Ne^{+}	2.317E−03	1.742E−02	6.205E−02	4.216E+00	2.709E+01	5.806E+01	0.000E+00
Na^{2+}	1.839E−03	3.921E−02	1.381E−01	3.130E+01	4.903E+01	1.871E+02	0.000E+00
Mg^{3+}	2.292E−02	9.832E−02	2.766E−01	1.488E+01	3.898E+01	7.846E+01	0.000E+00
Al^{4+}	2.144E−02	1.545E−01	8.548E−01	3.763E+00	3.457E+01	5.613E+01	1.087E+02
Si^{5+}	1.893E−02	2.233E−01	7.974E−01	1.230E+01	4.773E+01	1.127E+02	1.541E+02
P^{6+}	6.087E−02	3.903E−01	1.180E+00	2.434E+01	5.611E+01	1.474E+02	1.978E+02
S^{7+}	1.100E−01	5.151E−01	1.807E+00	1.975E+01	6.872E+01	2.047E+02	0.000E+00
Cl^{8+}	6.821E−02	6.112E−01	3.606E+00	2.161E+01	6.207E+01	1.175E+02	2.504E+02
Ar^{9+}	1.795E−01	9.445E−01	4.308E+00	3.652E+01	1.050E+02	2.882E+02	0.000E+00
K^{10+}	1.246E−01	9.901E−01	3.805E+00	4.429E+01	1.375E+02	3.373E+02	0.000E+00
Ca^{11+}	3.487E−01	1.391E+00	6.364E+00	4.594E+01	1.505E+02	3.797E+02	8.001E+03
Sc^{12+}	2.764E−01	1.599E+00	8.401E+00	5.409E+01	1.786E+02	4.323E+02	0.000E+00
Ti^{13+}	2.154E−01	1.384E+00	8.616E+00	7.174E+01	2.433E+02	4.964E+02	0.000E+00
V^{14+}	6.591E−01	2.141E+00	1.038E+01	7.603E+01	2.864E+02	5.625E+02	0.000E+00
Cr^{15+}	3.014E−01	2.375E+00	1.195E+01	7.835E+01	3.137E+02	6.161E+02	0.000E+00
Mn^{16+}	8.220E−01	3.207E+00	1.635E+01	8.841E+01	3.620E+02	6.978E+02	0.000E+00
Fe^{17+}	5.485E−01	3.311E+00	1.725E+01	9.910E+01	4.081E+02	7.662E+02	0.000E+00
Co^{18+}	1.480E+00	5.079E+00	1.728E+01	1.112E+02	4.148E+02	8.167E+02	0.000E+00
Ni^{19+}	4.095E−01	4.833E+00	1.560E+01	1.204E+02	4.341E+02	8.798E+02	0.000E+00
Cu^{20+}	2.189E+00	5.994E+00	2.048E+01	1.263E+02	5.171E+02	9.867E+02	0.000E+00
Zn^{21+}	7.219E−01	3.115E+00	2.211E+01	1.349E+02	6.398E+02	1.192E+03	0.000E+00
Kr^{27+}	1.366E+00	1.196E+01	3.538E+01	2.175E+02	8.541E+02	1.670E+03	0.000E+00
Mo^{33+}	1.163E+00	1.148E+01	7.714E+01	3.422E+02	1.173E+03	2.339E+03	0.000E+00
Xe^{45+}	3.746E+00	2.239E+01	1.559E+02	6.412E+02	2.156E+03	4.461E+03	0.000E+00

fitting parameters c_i and E_i for each member of the fluorine-like sequence. The fits reproduce our rate coefficient data to within 3% for 10^{-3} eV $< T/q^2 < 10^{+3}$ eV, where q is the residual charge of the initial F-like ion.

AUTOSTRUCTURE is implemented within the ADAS suite of programs as ADAS701. It produces raw autoionization and radiative rates which must be post-processed to obtain the final-state level-resolved and total DR rate coefficients. The post-processor ADASDR is used to reorganize the resultant data and also to add in radiative transitions between highly-excited Rydberg states, which are computed hydrogenically. This post-processor outputs directly the *adf09* file necessary for use by ADAS. The *adf09* files generated by our calculations in the intermediate coupling, configuration interaction approximation are available electronically (`http://www-cfadc.phy.ornl.gov/data_and_codes`). This site has tabulated DR rate coefficients into final LSJ levels from both the ground and metastable states in a manner useful to fusion and astrophysical modelers. Separate files *adf09* are produced for the excitations $2 \rightarrow 2$, $2 \rightarrow 3$ (capture to $n = 3$), and $2 \rightarrow 3$ (capture to $n > 3$), and are thus amenable to selective upgrade.

3. Results

Because of the complexity of the theoretical description for the DR process, it is almost impossible to say a priori which approximations in the calculations are justified and which are not. Laboratory measurements are needed to ensure that even state-of-the-art techniques produce reliable results. Before carrying out systematic calculations of DR rate coefficients for a whole sequence, we therefore first checked the chosen approximations by comparing to the available experimental data. Figure 1 presents the comparison of our MCBP DR rate coefficients with results of measurements using the heavy-ion TSR in Heidelberg (Savin et al. 1997, 1999) for Fe^{17+} to Fe^{16+} recombination. The cooler electrons employed in this technique have an anisotropic Maxwellian distribution with low perpendicular and parallel temperatures of $k_B T_\perp \approx 15$ meV and $k_B T_\parallel \approx 0.15$ meV, and allow resolution of separated resonances associated with $2 \rightarrow 2$ core excitation. These measurements therefore allow a very detailed comparison for the DR process. As seen in Fig. 1, our calculations based on the MCBP method in the isolated-resonance approximation reproduce all the main resonances and their intensities well. Though the $2s^2 2p^5 \rightarrow 2s2p^6$ dipole transition of the core gives the main contribution to the total DR process, the contribution from the fine-structure $2p^5\ ^2P_{3/2} \rightarrow 2p^5\ ^2P_{1/2}$ excitation is also very important.

The Maxwellian DR rate coefficients for Fe^{17+} as a function of electron temperature are compared in Fig. 2 with experimentally derived results and other published theoretical results. The $2 \rightarrow 2$ rate coefficients shown in Fig. 2a exhibit two maxima corresponding to the $2p^5\ ^2P_{3/2} \rightarrow 2p^5\ ^2P_{1/2}$ and $2s^2 2p^5\ ^2P_{3/2} \rightarrow 2s2p^6\ ^2S_{1/2}$ core excitations. Our MCBP DR rate coefficients for $2 \rightarrow 2$ excitation agree closely with experimental results within the estimated experimental uncertainty of ≈20% for all temperatures except the low-temperature region where our results are ≈30% lower than the experimental data.

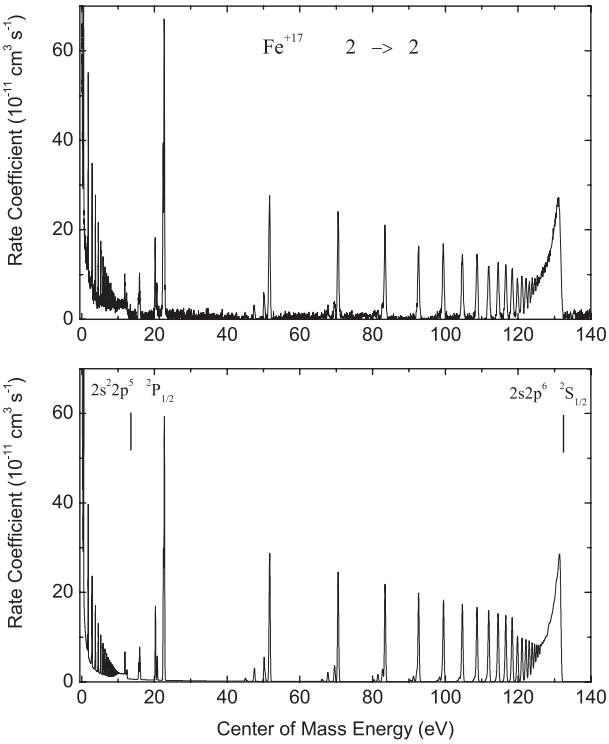

Fig. 1. Fe^{17+} to Fe^{16+} DR rate coefficients due to $2 \rightarrow 2$ core excitation: upper part, TSR experiment (Savin et al. 1997, 1999); bottom part, the present MCBP results. Also shown in the bottom plot are the series limits for DR via the $2s^2 2p^5\ ^2P_{1/2}$ and $2s2p^6\ ^2S_{1/2}$ core excitations.

The MCDF calculations by Chen (1988) underestimate the low temperature DR rate coefficient by a factor of ≈1.5. The single-configuration, LS-coupling calculations by Roszman (1987) overestimate the DR rate coefficient by a factor of ≈1.6 for temperatures above ≈30 eV. The single-configuration, intermediate-coupling results of Dasgupta & Whitney (1990) agree very well with the experimental results in the high temperature region. The recent MCDF results of Savin et al. (1997, 1999) agree with the experimental data as well as our MCBP results.

Figure 2b compares the total DR rate coefficients for Fe^{17+}. Also shown in Fig. 2 are the MCBP contributions from just the $2 \rightarrow 3$ core excitations. It characterizes the importance of the different processes in Eqs. (1) and (2) in the total DR rate coefficient. In an electron-ionized plasma, the peak in abundance of Fe^{17+} is predicted at $k_B T_e \approx 600$ eV (Mazzota et al. 1998). In this region, the main contribution to the total DR rate coefficient comes from the $2 \rightarrow 3$ core excitation.

As seen from Fig. 2, at low temperatures there is a large disagreement with the results of previous calculations which did not include contributions due to $2 \rightarrow 2$ $\Delta l = 0$ fine-structure core transitions shown in Eq. (1). Thus, they do not reproduce the correct low-temperature behavior for the DR rate coefficient, which is very important for modelling photoionized plasmas. At larger temperatures, there is large disagreement with the results from the simplified-model calculations of Jacobs et al. (1977). Closer agreement for larger temperatures is seen with the results of Roszman (1987) and Dasgupta & Whitney (1990). Our results are in excellent agreement with the

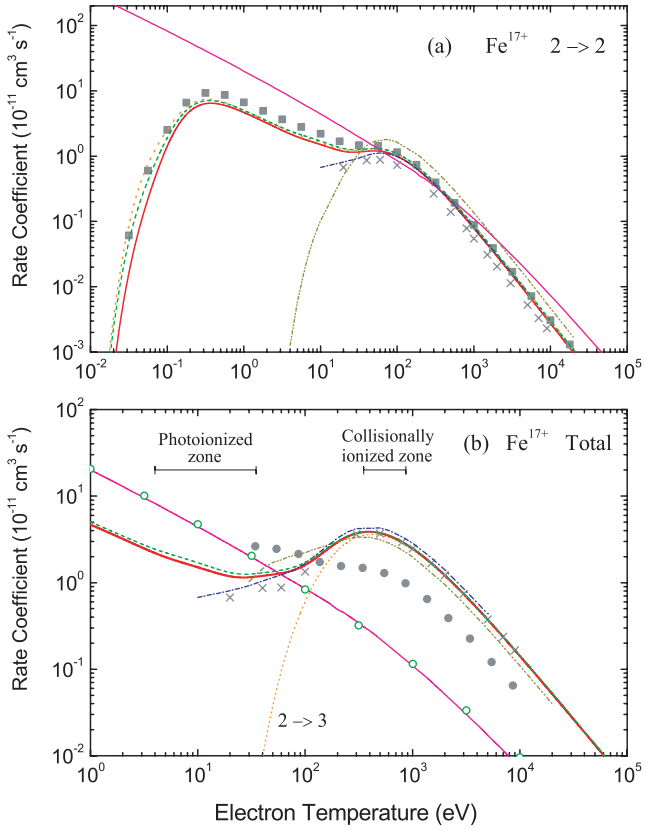

Fig. 2. Maxwellian-average DR rate coefficients for Fe^{17+} forming Fe^{16+} as a function of electron temperature (in eV). **a)** The $2 \rightarrow 2$ contribution. The *thick solid red curve* represents our MCBP results, the *solid squares* represent the experimentally derived rate coefficients (Savin et al. 1997, 1999), and the *thin solid magenta curve* shows the present MCBP radiative recombination rate coefficient. Comparison is given with the single-configuration LS-coupling results of Roszman (1987, *dot-dot-dashed dark yellow curve*) and Dasgupta & Whitney (1990, *dot-dashed blue curve*), with the MCDF results of Chen (1988, *crosses*) and Savin et al. (1997, 1999, *dotted orange curve*), and with the recent results of Gu (2003, *dashed green curve*). **b)** Total DR rate coefficient including both the $2 \rightarrow 2$ and $2 \rightarrow 3$ contributions. The labeling of the curves is the same as for **a)** except for the *dotted orange curve* which shows our MCBP contributions due to just the $2 \rightarrow 3$ core excitations. Also shown are the radiative recombination rate coefficients of Arnaud & Raymond (1992, *open circles*) and the simplified model calculations of Jacobs et al. (1977, *filled circles*).

MCDF results of Chen (1988). This highlights the importance of configuration interactions effects since these are included in the present calculations and those of Chen (1988) whereas they are absent in the single-configuration calculations of Roszman (1987) and Dasgupta & Whitney (1990).

An additional comparison with experimental data is presented in Fig. 3 for Se^{25+} (Lampert et al. 1996). These data also were obtained using the heavy-ion TSR. Our DR rate coefficients agree closely with the experimental results within the estimated experimental uncertainty of ≈15% for both $2 \rightarrow 2$ and for $2 \rightarrow 3$ core excitations. Our previous AUTOSTRUCTURE results (Lampert et al. 1996) were ≈20% below experiment for $\Delta N = 1$ DR. This previous work used semi-relativistic multiconfiguration Thomas-Fermi wavefunctions.

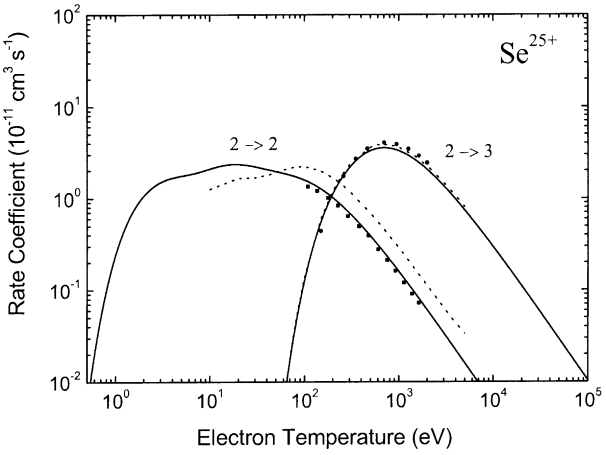

Fig. 3. The $2 \rightarrow 2$ and $2 \rightarrow 3$ DR rate coefficients for Se^{25+} forming Se^{24+} as a function of electron temperature (in eV). The solid curves represents our MCBP results, the solid squares and circles represent the experimentally derived rate coefficients for $2 \rightarrow 2$ and $2 \rightarrow 3$ DR, respectively (Lampert et al. 1996). Also shown is the LS-coupling HF results of Dasgupta & Whitney (1990, *dashed curve*).

Here, using non-relativistic multiconfiguration Hartree-Fock wavefunctions, our results are ≈10% higher than experiment for the $2 \rightarrow 2$ contribution, as seen in Fig. 3. We take this range in agreement between theory and experiment as a measure of the theoretical uncertainty which we estimate to be on the order of ±20%. The single-configuration calculations of Dasgupta & Whitney (1990) reproduce the $2 \rightarrow 3$ DR rate coefficients quite well, but overestimate the $2 \rightarrow 2$ DR rate coefficient by a factor of ≈1.7.

In Table 1, we present the fitting parameters for total DR rate coefficients for each ion from Ne^{+} to Zn^{21+}, and also for highly-charged ions Kr^{27+}, Mo^{33+}, and Xe^{45+}. In previous works, numerical calculations have been performed only for some ions in the sequence and the DR rate coefficients for other ions are interpolated (or extrapolated) assuming smooth behavior of DR rate coefficients as a function of nuclear charge (this approach was adopted in the work of Dasgupta & Whitney 1990). However, we have found that such analytic interpolations are applicable for the $2 \rightarrow 3$ DR rates, which scale smoothly as a function of Z (see Fig. 4a), but not for the $2 \rightarrow 2$ DR rates, which behave rather irregularly, especially at lower temperatures, as a function of Z (see Fig. 4b). The irregular $2 \rightarrow 2$ behavior is due to the shifting of intermediate states from just above threshold to just below threshold for certain adjacent values of Z; the shifted, bound intermediate state is no longer is accessible in the initial continuum, so it does not contribute to DR and the low-temperature DR rate coefficient is therefore decreased. As Z is increased further, a higher-lying resonance eventually moves to lower energies and the low-temperature DR rate coefficient is increased again.

An additional comparison of the earlier theoretical predictions with our results is given in Figs. 5 and 6. All previous calculations (except for Savin et al. 1997, 1999; and Gu 2003) failed to predict the large DR rate coefficients at small temperatures due to neglect of contributions from the fine-structure ($2p_{1/2}$–$2p_{3/2}$) excitation of the recombining ions. For

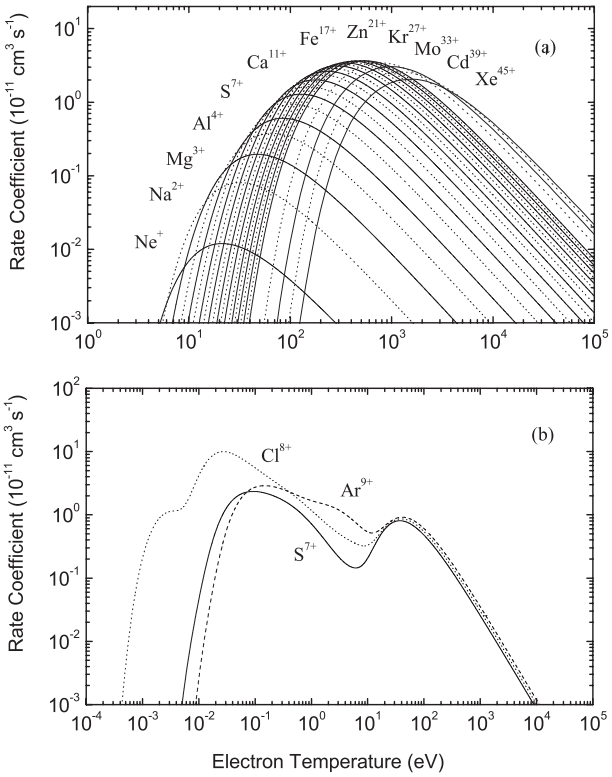

Fig. 4. Behavior of DR rate coefficients as a function of atomic number. **a)** Rate coefficients for $2 \rightarrow 3$ DR. Not all ions are labeled. **b)** Rate coefficients for $2 \rightarrow 2$ DR showing irregular dependence on Z.

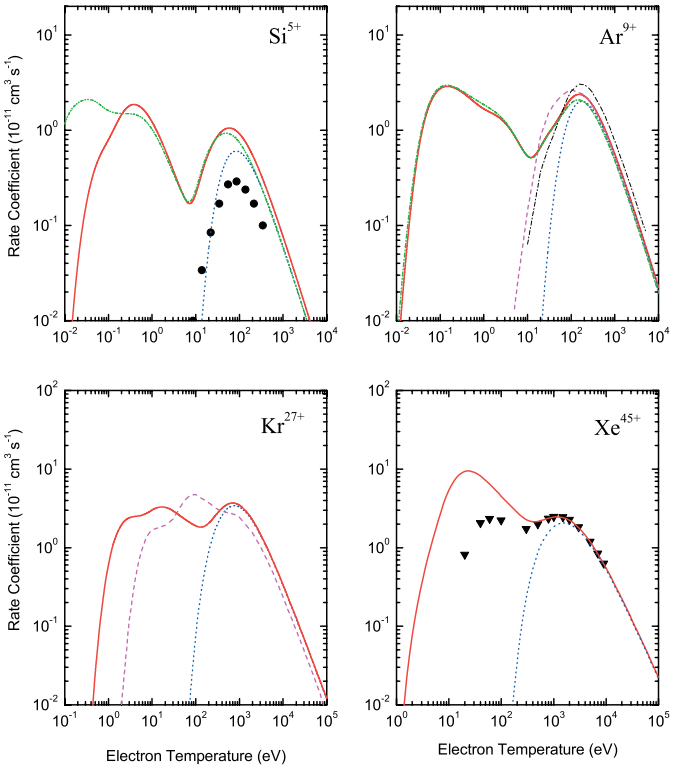

Fig. 5. Our DR rate coefficients for Si^{5+}, Ar^{9+}, Kr^{27+} and Xe^{45+} (*solid red curve*) as compared with results of Jacobs et al. (1979, *solid circles*), Roszman (1987, *dashed magenta curves*), Chen (1988, *solid triangles*), Dasguspa & Whitney (1990, *dot-dashed black curve*) and Gu (2003, *dot-dot-dashed green curve*). For comparison also shown in each plot is the $2 \rightarrow 3$ contribution (*dotted blue curve*).

low-charged ions, we found large discrepancies with the results of the simplified-model calculations of Jacobs et al. (1977), by a factor of ≈4 at the high temperature peak. The agreement with the HF results of Roszman (1987) and Dasgupta & Whitney (1990) is within 50% for the higher temperature region, but there are large discrepancies at lower temperatures due to an inaccurate representation of the low-lying resonances in a single-configuration model. On the other hand, we find excellent agreement with the MCDF results of Chen (1988) in the high temperature region for highly-charged ions. Both our MCBP calculations and the MCDF calculations, which are based on the Dirac equation, include relativistic effects whereas the HF calculations of Roszman (1987) and Dasgupta & Whitney (1990) do not, indicating that relativistic effects are quite important at lower temperatures. Good agreement with the recent results of Gu (2003) also confirms the reliability of the present results. In the case of Ar^{9+}, our data agree fairly closely with the results of Gu (2003) for all temperatures; noticeable discrepancies were found only for low temperature in the case of Si^{5+} and Ni^{19+}. As indicated by Gu (2003), the rate coefficient below 0.1 eV should be used with extra caution due to the limited accuracy of the low-lying resonance energies.

An overall comparison of our results with earlier theoretical predictions and with results from the recent critical compilation of Mazzota et al. (1998) is given in Fig. 7. Here we compare the high-temperature maxima of the various DR rate coefficients. For low-charged ions from Ne to Cl, the fitting data of Mazzota et al. (1998) are based on the simplified-model calculations of Jacobs et al. (1977, 1979) as fitted by Shull & Van Steenberg (1982), and considerably underestimate the DR rate coefficients. For the Ar-Ni ions, they adopted the fitting formula of Dasgupta & Whitney (1990), and here their DR rate coefficients are considerably higher than our results. Except for Mo^{33+}, there are large discrepancies with the DR rate coefficients of Roszman (1977). Closest agreement is found between our MCBP results and the MCDF results of Chen (1988) for highly-charged ions, and between our results and those of of Gu (2003) for lower-charged ions. We conclude that the compilation of Mazzota et al. (1998), which is based on results obtained with different methods and in different approximations, is problematic. The above comparisons emphasize the need for a systematic generation of data along an entire isoelectronic series.

4. Summary

In this paper, we have systematically calculated partial and total DR rate coefficients along the fluorine-like sequence as part of an assembly of a DR database necessary for the modelling of finite-density plasmas (Badnell et al. 2003). The approximations used for generating our data have been recently validated by the fairly good agreement of DR resonance strengths and energies between our theoretical data and the $2 \rightarrow 2$ experimental results from the Test Storage Ring in Heidelberg for fluorine-like Fe^{17+} (Savin et al. 1997, 1999) and

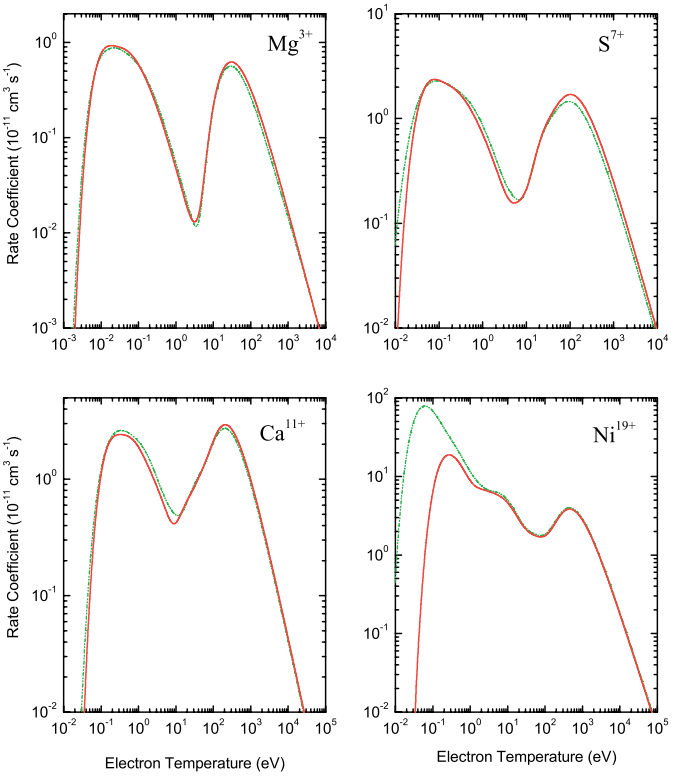

Fig. 6. Our DR rate coefficients for Mg^{3+}, S^{7+}, Ca^{11+}, and Ni^{19+} (*thick solid red curve*) as compared with results of Gu (2003, *dot-dot-dashed green curve*).

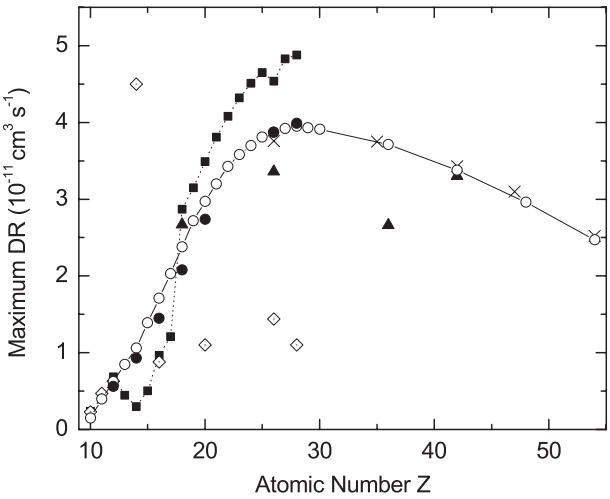

Fig. 7. Maximum total DR rate coefficients as a function of atomic number Z. The open circles represent our MCBP results. Comparison is given with simplified model calculation results of Jacobs et al. (1977, 1979, 1980, *open diamonds*) and Jacobs (1985, *open diamonds*); Hartree-Fock distorted-wave results of Roszman (1979, *up triangles*); compilation data of Mazzota et al. (1998, *solid squares*) based on the results of Jacobs et al. (1977, 1979, 1980) as fitted by Shull & van Steenberg (1982) and the HF calculations of Dasgupta & Whitney (1990); MCDF results of Chen (1988, *crosses*); and the recent results of Gu (2003, *solid circles*).

for both $2 \rightarrow 2$ and $2 \rightarrow 3$ experimental results for fluorine-like Se^{25+} (Lampert et al. 1996). Overall, we estimate the accuracy of our predicted DR rate coefficients to be $\approx \pm 20\%$ for temperatures above a few eV. We note, however, that storage ring results for Fe ions with different charge have demonstrated that all state-of-the-art theoretical methods (e.g., MCBP, MCDF, HULLAC, R-matrix, and FAC) are not able to reproduce reliably the DR resonance strengths and energies of L-shell ions for relative collision energies $\lesssim 1$ eV due to the limitations of the accuracies of the low-lying resonances theoretical energies (e.g., Savin et al. 1999; Schippers et al. 2001; Savin et al. 2002b; Schippers et al. 2004) due to the limitation of the accuracies of the low-lying resonance theoretical energies. The theoretical DR rate coefficients below ≈ 1 eV should be used with extra caution, and for reliable total DR rate coefficients at plasma temperatures where these resonances play a significant role, these MCBP results need to be supplemented with storage ring measurements of the relevant resonances.

We have presented selected total rate coefficients for some ions of interest and have made comparisons, where possible, with previous work. We found large disagreement with the results from previous calculations, including the fits from the recent critical compilation of Mazzotta et al. (1998), as had been found also by Gu (2003). Initial and final state resolved rate coefficients have been tabulated, and these data are available from the web site `http://www-cfadc.phy.ornl.gov/data_and_codes`. The total DR rate coefficients have been fitted by simple analytical formula, which will also prove of great use to astrophysical and fusion plasma modelers, and are available from our web sites `http://homepages.wmich.edu/~gorczyca/drdata` and `http://amdpp.phys.strath.ac.uk/tamoc/DR/`.

We have calculated our data over a wide temperature range and for a large number of atomic ions in order to maximize the available information for modelling work. The fits to our DR rate coefficients reproduce our DR data to better than 3% for all ions in the wide temperature range from 10^{-3} eV $< T/q^2 < 10^{+3}$ eV. These DR data are suitable for modelling of solar and cosmic plasmas under conditions of collisional ionization equilibrium, photoionization equilibrium, and non-equilibrium ionization. In the future, we will present dielectronic recombination data for further isoelectronic sequences as detailed previously (Badnell et al. 2003), see e.g. Altun et al. (2005) for the Na-like sequence.

Acknowledgements. TWG, KTK, OZ, and JF were supported in part by NASA Space Astrophysical Research and Analysis Program grant NAG5-10448 and NASA Astronomy and Physics Research and Analysis Program grant NNG0-4GB58G. TWG was also partially supported by the National Science Foundation through a grant for the Institute for Theoretical Atomic and Molecular Physics at Harvard University and Smithsonian Astrophysical Observatory. DWS was supported in part by NASA Space Astrophysical Research and Analysis Program grant NAG5-5420 and NASA Solar and Heliospheric Supporting Research & Technology grant NAG5-12798.

References

Altun, Z., Yumak, A., Badnell, N. R., et al. 2005, A&A, submitted
Arnaud, M., & Raymond, J. 1992, ApJ, 398, 396
Badnell, N. R. 1986, J. Phys. B, 19, 3827

Badnell, N. R. 1997, J. Phys. B, 30, 1
Badnell, N. R., & Pindzola, M. S. 1989, Phys. Rev. A 39, 1690
Badnell, N. R., O'Mullane, M., Summers, H. P., et al. 2003, A&A, 406, 1151
Bar-Shalom, A., Klapish, M., & Oreg, J. 2001, J. Quant. Spectrosc. Radiat. Transfer, 71, 169
Chen, M. H. 1988, Phys. Rev. A, 38, 2332
Dasgupta, A., & Whitney, K. G. 1990, Phys. Rev. A, 42, 2640
Froese Fisher, C. 1991, Comput. Phys. Commun., 64, 369
Gorczyca, T. W., Robicheaux, F., Pindzola, M. S., & Badnell, N. R. 1995, Phys. Rev. A, 52, 3852
Gorczyca, T. W., Robicheaux, F., Pindzola, M. S., & Badnell, N. R. 1996, Phys. Rev. A, 54, 2107
Gorczyca, T. W., Badnell, N. R., & Savin, D. W. 2002, Phys. Rev. A, 65, 062707
Gu, M. F. 2003, ApJ, 590, 1131
Jacobs, V. L. 1985, ApJ, 296, 121; erratum 299, 1079
Jacobs, V. L., Davis, J., Kepple, P. C., & Bhala, M. 1977, ApJ, 211, 605, 215, 690
Jacobs, V. L., Davis, J., Kepple, P. C., & Bhala, M. 1979, ApJ, 230, 627
Jacobs, V. L., Davis, J., Rogerson, J. E., et al. 1980, ApJ, 239, 1119
Lampert, A., Wolf, A., Habs, D., et al. 1996, Phys. Rev. A, 53, 1413
Mazzotta, P., Mazzitelli, G., Colafrancesco, S., & Vittorio, N. 1998, A&ASS, 133, 403
Mitnik, D. M., & Badnell, N. R. 2004, A&A, 425, 1153
Pindzola, M. S., Badnell, N. R., & Griffin, D. C. 1992, Phys. Rev. A, 46, 5725
Robicheaux, F., Gorczyca, T. W., Pindzola, M. S., & Badnell, N. R. 1995, Phys. Rev. A, 52, 1319
Roszman, L. J. 1987, Phys. Rev. A, 35, 2138
Savin, D. W., & Laming, J. M. 2002, ApJ, 566, 1166
Savin, D. W., Bartsch, T., Chen, M. H., et al. 1997, ApJ, 489, L115
Savin, D. W., Kahn, S. M., Linkemann, J., et al. 1999, ApJS, 123, 687
Savin, D. W., Kahn, S. M., Linkemann, J., et al. 2002a, ApJ, 576, 1098
Savin, D. W., Behar, E., Kahn, S. M., et al. 2002b, ApJS, 138, 337
Savin, D. W., Kahn, S. M., Gwinner, G., et al. 2003, ApJS, 147, 421
Schippers, S., Müller, A., Gwinner, G., et al. 2001, ApJ, 555, 1027
Schippers, S., Schnell, M., Brandau, C., et al. 2004, A&A, 421, 1185
Shull, J. M., & van Steenberg, M. 1982, ApJS, 46, 95
Summers, H. P. 2003, Atomic Data & Analysis Structure User Manual (version 2.7) – http://adas.phys.strath.ac.uk
Verner, D. A., & Ferland, G. J. 1996, ApJS, 103, 467
Zatsarinny, O., Gorczyca, T. W., Korista, K., Badnell, N. R., & Savin, D. W. 2004, A&A, 426, 699